Bioorganic & Medicinal Chemistry 21 (2013) 223–234

Contents lists available at SciVerse ScienceDirect

Bioorganic & Medicinal Chemistry

journal homepage: www.elsevier.com/locate/bmc

Bis(acridine-9-carboxylate)-nitro-europium(III) dihydrate complex a new apoptotic agent through Flk-1 down regulation, caspase-3 activation and oligonucleosomes DNA fragmentation

Hassan A. Azab [a], Belal H. M. Hussein [a,e], Mona F. El-Azab [b], Mohamed Gomaa [c], Abdullah I. El-Falouji [d,*]

[a] Chemistry Department, Faculty of Science, Suez Canal University, Ismailia 41522, Egypt
[b] Department of Pharmacology and Toxicology, Suez Canal University, Ismailia 41522, Egypt
[c] Medicinal Chemistry Department, Faculty of Pharmacy, Suez Canal University, Ismailia 41522, Egypt
[d] Biotechnology Research Center, Suez Canal University, Ismailia 41522, Egypt
[e] Chemistry Department, Faculty of Science&Art, Al Ula, Taibah University, KSA

A R T I C L E I N F O

Article history:
Received 7 August 2012
Revised 11 October 2012
Accepted 20 October 2012
Available online 27 October 2012

Keywords:
Bis(acridine-9-carboxylate)-nitro-europium(III) dihydrate complex
Apoptosis
Antitumor activity
Caspase-3
DNA fragmentation
Anti-angiogenesis

A B S T R A C T

New bis(acridine-9-carboxylate)-nitro-europium(III) dihydrate complex was synthesized and characterized. In vivo anti-angiogenic activities of bis(acridine-9-carboxylate)-nitro-europium(III) dihydrate complex against Ehrlich ascites carcinoma (EAC) cells are described. The newly synthesized complex resulted in inhibition of proliferation of EAC cells and ascites formation. The anti-tumor effect was found to be through anti-angiogenic activity as evident by the reduction of microvessel density in EAC solid tumors. The anti-angiogenic effect is mediated through down-regulation of VEGF receptor type-2 (Flk-1). The complex was also found to significantly increase the level of caspase-3 in laboratory animals compared to the acridine ligand and to the control group. This was also consistent with the DNA fragmentation detected by capillary electrophoresis that proved the apoptotic effect of the new complex. Our complex exhibited anti-angiogenic and apoptotic activity in vivo, a thing that makes it a potential effective chemotherapeutic agent. The interaction of calf thymus DNA (ct-DNA) with bis(acridine-9-carboxylate)-nitro-europium(III) dihydrate complex has been investigated using fluorescence technique. A competitive experiment of the europium(III)-acridine complex with ethidium bromide (EB) to bind DNA revealed that interaction between the europium(III)-acridine and DNA was via intercalation. The interaction of the synthesized complex with tyrosine kinases was also studied using molecular docking simulation to further substantiate its mode of action.

1. Introduction

Angiogenesis is a physiological process that is needed for tumor growth and metastasis formation. It is an extremely necessary process for tumor cells growth as it provides the oxygen and nutrient required.[1] Therefore, enormous researches have focused on the development of angiogenesis inhibitors that target tumor vasculature as anticancer drugs.[2–4]

Apoptosis is an essential cellular process that regulates and maintains the balance between proliferation, growth arrest and cell death. Apoptosis differs from necrosis in that it happens in a controlled and regulated manner. Specific signals trigger the process of apoptosis leading to a number of cellular biochemical and morphological changes. The chemotherapeutic cancer treatment through induction of apoptosis has now become one of the most important fields of anticancer research with considerable efforts being focusing on finding active selective and less toxic candidates.[5,6]

Recent preclinical studies showed synergistic action between apoptosis and anti-angiogenic therapy.[7–9] Belakavadi and Salimath [8] have also addressed the synergy between apoptosis and anti-angiogenesis through induction of caspase-3 and down regulation of VEGF expression, respectively. An improved efficacy in lung cancer progression has also been demonstrated through the combination of antiangiogenic and apoptotic effects.[9]

In recent years, one of the successful and effective approaches in the search for new chemotherapeutic agents is the development of new rare earth metals-based anti-cancer agents. A number of lanthanide complexes have been synthesized and the evaluation of their cytotoxic activities have revealed potential promising antitumor agents.[10–13]

Acridine and its derivatives are planar tricyclic aromatic molecules, with anticancer potential that was first noted in the 1920s. Since then, a large number of acridines have been tested as antitumor agents.[14–18] Moreover, some acridines have been used as

* Corresponding author. Tel.: +20 1115990299; fax: +20 64 3200452.
E-mail address: falouji@hotmail.com (A.I. El-Falouji).

0968-0896/$ - see front matter © 2012 Elsevier Ltd. All rights reserved.
http://dx.doi.org/10.1016/j.bmc.2012.10.020

antibacterial,[19] anti-malarial[20] and anti-inflammatory agents.[21] Also, Acridines can be interconverted relatively easily, a property that helped in the design of several synthetic compounds from acridine nucleus.[22,23]

In this work, a novel Eu(III) complex containing 9-acridine carboxylate (9-ACA) was synthesized and characterized. The anti-tumor effect of that complex against Ehrlich ascites tumor (EAC) cells was tested. The results showed an evidence that Eu(III)-complex containing 9-acridine carboxylate induced apoptosis in EAC cells through caspase-3 activation resulting in DNA fragmentation. Furthermore, an anti-angiogenic effect of that complex mediated by down-regulation of VEGF receptor type-2 (Flk-1) and CD31 was also observed**.** Carboplatin as a reference drug has been used in the current study. This drug has been proven to be significantly less in antiangiogenic activity and VEGFR (Flk-1) and CD31 agonist activity. The fluorescent ethidium bromide measurements were carried out to investigate the binding mechanism of bis(acridine-9-carboxylate)-nitro-europium(III) dihydrate complex with DNA. Knowing that Flk-1 is a tyrosine kinase receptor, molecular docking simulation was used to study the interaction of the complex with different tyrosine kinases known to be associated with cancer pathogenesis to further confirm the antiangiogenic activity of the complex.

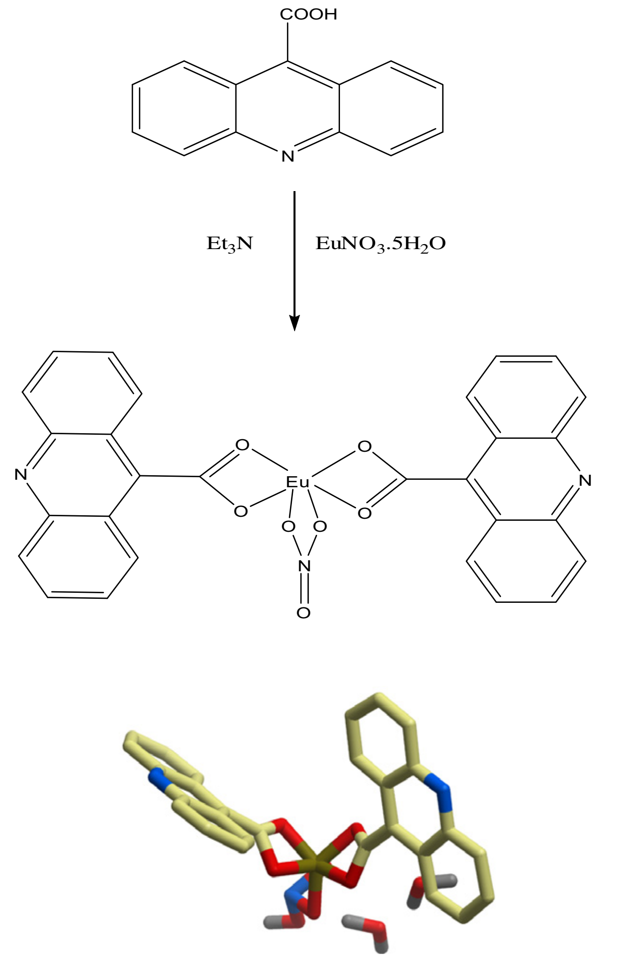

Scheme 1. Suggested structure of the Bis(acridine-9-carboxylate)-nitro-europium(III) dihydrate complex.

2. Experimental

2.1. Materials and reagents

$Eu(NO_3)_3{\cdot}5H_2O$ and 9-acridine carboxylic acid (9-ACA) were purchased from Sigma and used without further purification. Carboplatin was purchased from (MP Biomedicals, LLC, France). GF-1 DNA Extraction Kit was purchased from Vivantis. Primary antibody Flk-1 was purchased from (Santa Cruz Biotechnology, CA, USA), anti-CD31 Class II was purchased from (Dako cytomation, Carpinteria, USA), caspase-3 antibody was purchased from (Thermo Fisher Scientific, UK). DNA concentrations were determined by absorption spectroscopy using the molar coefficient of 6600 $M^{-1}cm^{-1}$ at the wavelength of 260 nm. A solution of ct-DNA in the buffer gave a ratio of UV absorbance of about 1.89 at 260 and 280 nm, indicating that the ct-DNA was sufficiently free of protein.

2.2. Apparatus

Fluorescence spectra of ethidium bromide displacement were carried out with Jasco-6300 spectrofluorometer equipped with a 150 W xenon lamp source and quartz cells of 1 cm path length. The slit widths of excitation and emission wavelength were 5 nm/5 nm. Elemental analysis was carried out by Elementar vario; thermogravimetric analysis was carried out by (a Shimazdu TGDTA). ^{1}H and ^{13}C NMR spectra were recorded on a Joel-400 NMR, Mass spectrometry was carried out by Shimazdu Qp-2010 plus mass analyzer, elemental analysis was carried out by elementar vario, the infrared spectra were obtained in the 4000–400 cm^{-1} region by using Bruker Alpha with KBr discs. Melting point was determined on a MEL-TEMP II apparatus. Nanodrop spectrophotometer model ND 1000 was used for measuring DNA concentrations. Multi-capillary electrophoresis QIAxcel (QIAGEN Germany) system was used for DNA fragmentation analysis.

2.3. Synthesis and characterization of bis(acridine-9-carboxylate)-nitro-europium(III) dihydrate complex

The 9-acridine carboxylic acid (1.0 mmol, 0.224 g) was dissolved in ethanol (20 mL) and triethylamine (1.0 mmol, 0.102 g) was then added. The solution was stirred for 15 min at room temperature. $Eu(III)(NO_3)_3{\cdot}5H_2O$ (0.5 mmol) was dissolved in 20 mL ethanol and then added slowly with vigorous stirring to the 9-acridine carboxylic acid solution. The precipitate appeared immediately after mixing the two solutions. Then the mixture was allowed to stir overnight at room temperature. This product was collected by filtration, purified by washing several times with hot ethanol and dried in vacuum over P_4O_{10}. The structure of Eu(III) complex as suggested in Scheme 1 was confirmed from analytical analysis, ^{1}H NMR, ^{13}C NMR, IR spectroscopic methods, and thermal analysis.

2.4. Tumor cell line

Ehrlich ascites carcinoma (EAC) cell line was purchased from the Tumor Biology Department, National Cancer Institute, Cairo University (Cairo, Egypt). EAC is a murine spontaneous breast cancer from which an ascites variant was obtained. The tumor cell line was maintained in our laboratory by serial intraperitoneal (ip) passage in female Swiss albino mice at 7–10 day interval. Tumor cells were tested for viability and contamination using trypan blue dye exclusion technique.[24]

2.5. In vivo anti-tumor activity

2.5.1. Experimental animals

All animal procedures and experimental protocols were carried out in accordance with the guide for the care and use of laboratory animals. Swiss albino mice weighing 20–25 g were obtained from the Egyptian organization for biological products and vaccines (Vacsera, Egypt). They were housed under controlled conditions (25 ± 1 °C, constant temperature, 55% relative humidity, and 12 h dark/light cycles), food and water were allowed *ad libitum* throughout the study period.

2.5.2. Induction of solid tumors

EAC cells were suspended in normal saline so that each 100 µl contains 2.5×10^6 cells. Each mouse was inoculated intradermally (id) at 2 sites bilaterally on the lower ventral side with 100 µl EAC suspension on each site.[25]

2.5.3. Induction of ascites

In a parallel experiment, mice were injected intraperitoneally (ip) with 100 µl EAC suspension (5×10^6 cells)/mouse to induce ascites. These mice received the same pharmacological treatment as explained below.[8,26–28] At the end of the experiment, the ascites fluids were collected and divided into two portions, the 1st portion was immediately snap frozen in liquid nitrogen for the DNA extraction and the other portion was used for the determination of EAC cell counts.

2.5.4. Pharmacological treatment

The mice were randomly assigned into 3 main groups, 8 mice each. The first group received vehicle injection (DMSO in PBS) and served as control. Second and third groups were injected daily with 5 mg/kg (ip) of 9-acridine carboxylic acid or bis(acridine-9-carboxylate)-nitro-europium(III) dihydrate complex, respectively. The complex was dissolved in 10% DMSO:PBS v/v the concentration used is 5 mg/kg and the injected volume was 100 µl. All treatments started 6 days after tumor cells inoculation.[26–28] At the end of the experiment, mice were sacrificed by cervical dislocation then tumors were excised and fixed in 10% neutral buffered formalin.

2.5.5. DNA extraction

DNA was purified from Ehrlich ascites carcinoma cells using the GF-1 DNA extraction kit (*Vivantis*). DNA fragments were analyzed in the automatic multi-capillary electrophoresis QIAxcel system. Isolated DNA was placed in the instrument sample tray, 10 µl of the DNA samples were automatically injected into the capillary channel and subjected to electrophoresis according to the protocol AM320 (applied separation time: 323 s, method separation time: 320 s, method injection time: 10 s, method separation voltage: 6.0 kV and method injection voltage: 5.0 kV) of the QIAxcel DNA Screening Kit.

2.5.6. Immunohistochemistry

Sections were cut into 4 µl then fixed in a 65 °C oven for 1 h. Triology (Cell Marque, CA-USA. cat# 920p-06) is a product that combines the three pretreatment steps: deparaffinization, rehydration and unmasking. Using this product enhances standardization of the pretreatment procedure, thereby producing more consistent, more reliable results. Slides were placed in a coplin jar filled with 60 mL of triology working solution and the jar is securely positioned in the autoclave. The autoclave was adjusted so that temperature reached 120 °C and maintained stable for 15 min after which pressure was released and the coplin jar was removed to allow slides to cool for 30 min. Sections were then washed and immersed in TBS to adjust the pH, this is repeated between each step of the IHC procedure. Quenching endogenous peroxidase activity was performed by immersing slides in 3% hydrogen peroxide for 10 min. Broad spectrum LAB-SA detection system from Invitrogen (Cat# 85-9043) was used to visualize any antigen-antibody reaction in the tissues. Background staining was blocked by putting 2–3 drops of 10% goat non immune serum on each slide and incubating them in a humidity chamber for 10 min. Without washing, excess serum was drained from each slide and 2–3 drops of the ready to use primary mouse antibody Flk-1, anti-CD31 Class II and anti-caspase-3 were applied, then slides were incubated in the humidity chamber for 1 h. Henceforward, biotinylated secondary antibody was applied on each slide for 20 min followed by 20 min incubation with the enzyme conjugate. DAB chromogen was prepared and 2–3 drops were applied on each slide for 2 min. DAB was rinsed, after which counterstaining and cover slipping were performed as the final step before slides were examined under the light microscope.

2.5.7. Tumor mass

All tumors, 2-discs/animal, were punched out, weighed immediately, and the average weight was calculated. All tumors were then kept in 10% neutral buffered formalin for histological evaluation.

2.6. Cytotoxicity assay in vitro

Standard MTT assay procedures was used to test the cytotoxicity of the bis(acridine-9-carboxylate)-nitro-europium(III) dihydrate complex and 9-acridine carboxylic acid ligand.[29] Cells were grown as monolayer in Eagle's minimum essential medium (MEM) with 10% inactivated fetal calf serum and 50 µg/mL gentamicin in 96-well microassay culture plates (10×10^3 cells per well) and grown for 24 h at 37 °C in a humidified incubator with 5% CO_2. Control wells were prepared by addition of culture medium and cisplatin were used as negative and positive control, respectively.

The monolayers were then washed with sterile phosphate buffered saline (0.01 M pH 7.2) and simultaneously the cells were treated with 100 µl from different concentration (1–50 µM) from the bis(acridine-9-carboxylate)-nitro-europium(III) dihydrate complex and 9-acridine carboxylic acid ligand in fresh maintenance medium and incubated at 37 °C. Six wells were used for each concentration of the tested compounds. After 24 h the number of cells was determined using the MTT assay and read the absorbance at 590 nm using ELISA reader and the absorbance reading of the untreated cells were considered as 100% proliferation.

2.7. Quantification of immunohistochemistry

For quantitative analysis, the area percentage of immunoreactive cells was used as a criterion of cellular activity after substracting background noise. Measurement was done using an image analyzer (ImageJ programme, 1.41a, NIH, USA). From each slide of all experimental groups, seven fields were randomly selected; area percentage of nine random parts within each field was analyzed and the mean for them was expressed as field area percent. The average of the seven fields was obtained for each slide.

2.8. Data analysis

Statistics were calculated with graph pad for windows version 5.0, the mean values obtained in the different groups were compared by one way ANOVA followed by Tukey multiple comparison test. All results were expressed as mean values ± SD. A P value $\leqslant 0.05$ was considered statistically significant.

2.9. Molecular modeling

All molecular modeling studies were performed on a Hewlett-Packard Pentium Dual-Core T4300 2.10 GHz running Windows 7 Ultimate using molecular operating environment (MOE) 2008.10[30] molecular modeling software. The studied enzymes and DNA are all crystal structure determined by X-ray crystallography to a high resolution and co-crystallized with inhibitors. The 3D structure of these enzymes and DNA were downloaded in PDB format from the Protein Data Bank (PDB) website[31] and used in the docking studies.

The docking studies were performed after deleting the co-crystallized inhibitors from the active site. Ligands were then docked within the active site of the crystallized structures using MOE dock tool in MOE, performed with the default values. The active site was defined by all the amino acid residues involved in the interaction with the co-crystallized inhibitors. The output databases of MOE docking were checked and evaluated visually for any interactions established between the active site and the proposed inhibitors. The docking pose of the proposed inhibitors were also compared to that of the known co-crystallized inhibitors.

3. Result

3.1. Chemistry of bis(acridine-9-carboxylate)-nitro-europium(III) dihydrate complex

The bis(acridine-9-carboxylate)-nitro-europium(III) dihydrate complex was synthesized through the reaction of acridine-9-carboxylic acid and europium nitrate penthydrate in the presence of triethylamine in ethanol at room temperature. The reaction mixture was stirred overnight and the precipitate formed was filtered and dried over phosphorous pentoxide. The complex is air stable for extended periods and soluble in DMSO and DMF; insoluble in alcohol, benzene, water, and diethyl ether. Because of the insolubility of the complex in suitable solvents we were unsuccessful in growing crystals for single crystal X-ray structural studies. The molar conductance value is 26 $ohm^{-1}\,mol^{-1}\,cm^2$ in DMF, showing that the Eu(III) complex is non-electrolytic in DMF. The molar conductance of $Eu(NO_3)_3$ was measured and was found to be 412 $ohm^{-1}\,mol^{-1}\,cm^2$. The low molar conductance of the synthesized compound suggested that a complex is formed rather than a salt. The elemental analysis suggests that the formula of the complex is $[Eu\,(9\text{-}ACA)_2(NO_3)]\cdot 2H_2O$, mp: over 300 °C; elemental analysis calculated (%): C, 48.28; H, 2.87; N, 4.02; Eu(III) 21.8; found: C, 48.54; H, 3.1; N, 4.9; Eu(III) 20.04.

3.1.1. Thermal analysis

The thermal decomposition of the $[Eu(9\text{-}ACA)_2(NO_3)]\cdot 2H_2O$ complex was studied using the thermogravimetric (TG) and differential thermal analysis (DTA) techniques. The experiment was performed under N_2 atmosphere with a heating rate of 10 °C/min in the temperature range of 25–800 °C. The TG curve exhibits many steps of weight losses. The first mass loss is due to dehydration with loss of non coordinating water ($2H_2O$; calculated = 5.17%; found = 5.22%). The appearance of the endothermic peaks on the DTA curve observed at 48.5 °C could be confirmed as phase transition. The second weight loss peak occurred at 210 °C combined with endothermic peak could be due to the removal of nitrate (calculated = 8.91%; found = 8.22%). The third significant weight loss of 65.51% occurred at 491 °C corresponding to the decarboxylation and decomposition of 9-ACA ligand (calculated: 64.08%; found = 65.51%). The decomposition of 9-ACA was ac companied by strong endothermic peak on DTA curve. The remaining weight of 24.84% corresponds to the final thermal decomposition residue is Eu_2O_3.

3.1.2. Infrared spectra

In the IR spectral data ligand of 9-ACA showed that, broad and weak bands centered at 3445 cm^{-1} which can be attributed to the OH group. In addition, the high strong sharp band which observed at 1651 cm^{-1} could be referred to the C=O group. The strong band which appeared at 1606 cm^{-1} was assigned to C=C of aromatic ring. The Eu(III) complex exhibited broad weak band centered at 3365 cm^{-1}, which could be assigned as the stretching band for the water molecules. The strong band which appeared at 1651 cm^{-1} in 9-ACA, which was ascribed to C=O, gave downshift to 1553 cm^{-1} in the Eu(III) complex. This emphasizes that the involvement of the of C=O group in the chelation process of the Eu(III) complex. The complex showed a medium band at 417 cm^{-1} which could be assigned as stretching of the Eu–O bound. The bands around 1520 and 1300 cm^{-1} which assigned as stretching vibration of nitrate group were splitted by 240 cm^{-1} which indicate the bidentate nature of the nitrate group.

3.1.3. Mass spectroscopic studies

The interpretation of the mass experiment results showed the molecular ion peak (M^+) at 694 m/z which correspond to the molecular weight of the proposed bis(acridine-9-carboxylate)-nitro-europium(III) dihydrate complex $[Eu(9\text{-}ACA)_2(NO_3)]\cdot 2H_2O$. Other peaks at 658 and 596 m/z are due to M-$2H_2O$, and M-(NO_3 + $2H_2O$), corresponding to the loss of the two molecules of water of hydration and nitrate group, respectively. Other fragmentation peaks were corresponding to the acridine-9-carboxylate which was found not very useful in confirming the structure of the complex.

3.1.4. ^{1}H and ^{13}C NMR spectra

The ^{1}H NMR spectra of 9-ACA and its bis(acridine-9-carboxylate)-nitro-europium(III) dihydrate were measured and analyzed to confirm the complex formation. The chemical shifts of the ^{1}H NMR spectra in DMSO-d_6 were presented as follows: 9-ACA: ^{1}H NMR (DMSO-d_6): 8.68 (s, 1H, H10), 7.83 (d, J = 8.1, 2H, H1, H9), 7.67 (d, J = 8.2, 2H, H4, H6), 7.38 (m, 2H, H2, H8), 7.32 (m, 2H, H3, H7); Eu-(9-ACA)2 complex: ^{1}H NMR (DMSO-d_6): 7.71 (d, J = 7.9, 4H, H1, H9), 7.67 (d, J = 8.0, 4H, H4, H6), 7.24 (m, 4H, H2, H8), 7.21 (m, 4H, H3, H7). ^{13}C NMR (DMSO-d_6: ppm): 163.51 (C=O), 148.64 (N–C), 131.95 (C–C=O), 130.2 (C-Ar), 129.1 (C-Ar), 124.15 (C-Ar), 122.96 (C-Ar), and 121.4 (C-Ar). A survey of the spectral data reveals slight change in chemical shifts of the ^{1}H in the Eu(III) complex spectrum relative to the free ligand. The carboxylic proton (8.68 ppm) peak was absent in the spectrum of the complex due to the deprotonation of the carboxylic group.

3.2. Bis(acridine-9-carboxylate)-nitro-europium(III) dihydrate complex inhibits tumor proliferation and decreases the ascites secretion from EAC cells in vivo

To determine the in vivo effect of bis(acridine-9-carboxylate)-nitro-europium(III) dihydrate complex on tumor cell growth, ehrlich ascites carcinoma cells (EACs) were treated with bis(acridine-9-carboxylate)-nitro-europium(III) dihydrate complex, Carboplatin or acridine-9-carboxylic acid only. As shown in Figure 1(B), single treatment with bis(acridine-9-carboxylate)-nitro-europium(III) dihydrate complex produced a significant reduction ($P \leqslant 0.05$) in tumor mass on day 14 post-inoculation as compared to carboplatin, acridine-9-carboxylic acid, and untreated control animals.

Moreover, reduction of ascites formation by treatment with bis(acridine-9-carboxylate)-nitro-europium(III) dihydrate complex was confirmed using trypan blue exclusion method.[24] As shown in Figure 1(B), single treatment with bis(acridine-9-carboxylate)-nitro-europium(III) dihydrate complex significantly reduced the number of EAC cells ($P \leqslant 0.05$) after 7 days of treatment as compared to the acridine-9-carboxylic acid treated group, carboplatin as well as untreated control animals.

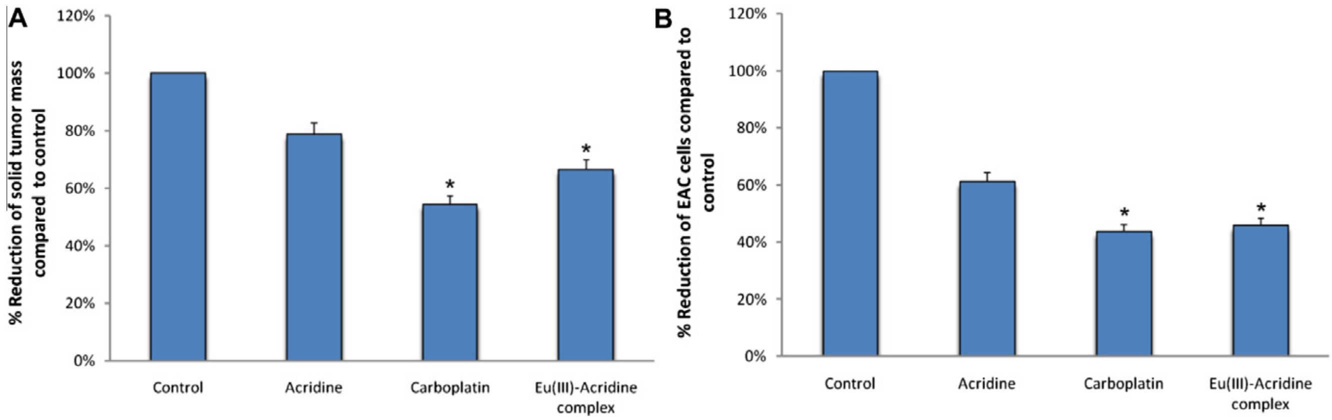

Figure 1. (A) Statistical analysis of the $[Eu(9\text{-}ACA)_2(NO_3)]\cdot 2H_2O$ complex treatment on solid tumor mass. (B) Statistical analysis of the $[Eu(9\text{-}ACA)_2(NO_3)]\cdot 2H_2O$ complex treatment on number of Ehrlich ascites carcinoma cells (EACs). Data represent mean ± S.E.

3.3. Effect of bis(acridine-9-carboxylate)-nitro-europium(III) dihydrate complex on tumor angiogenesis

To investigate the effect of the newly synthesized compound on the tumor angiogenesis, the expression of CD31 and VEGF receptor type-2 (Flk-1) were evaluated.

CD31, or platelet endothelial cell adhesion molecule-1 (PE-CAM-1), is found in large quantities on the surface of endothelial cells (ECs) and is less abundant on platelets and leukocytes. It plays a major role in a number of cellular interactions, particularly in adhesion between ECs and polymorphonuclear leukocytes, monocytes, and lymphocytes during inflammation, and between adjacent ECs during angiogenesis.[32,33] By examining the immunohistochemical staining for CD31 of tumor sections from the control and treated groups, a marked decrease of immunohistochemical staining of the CD31 was observed in the treated group in comparison to control group as shown in Figure 2A.

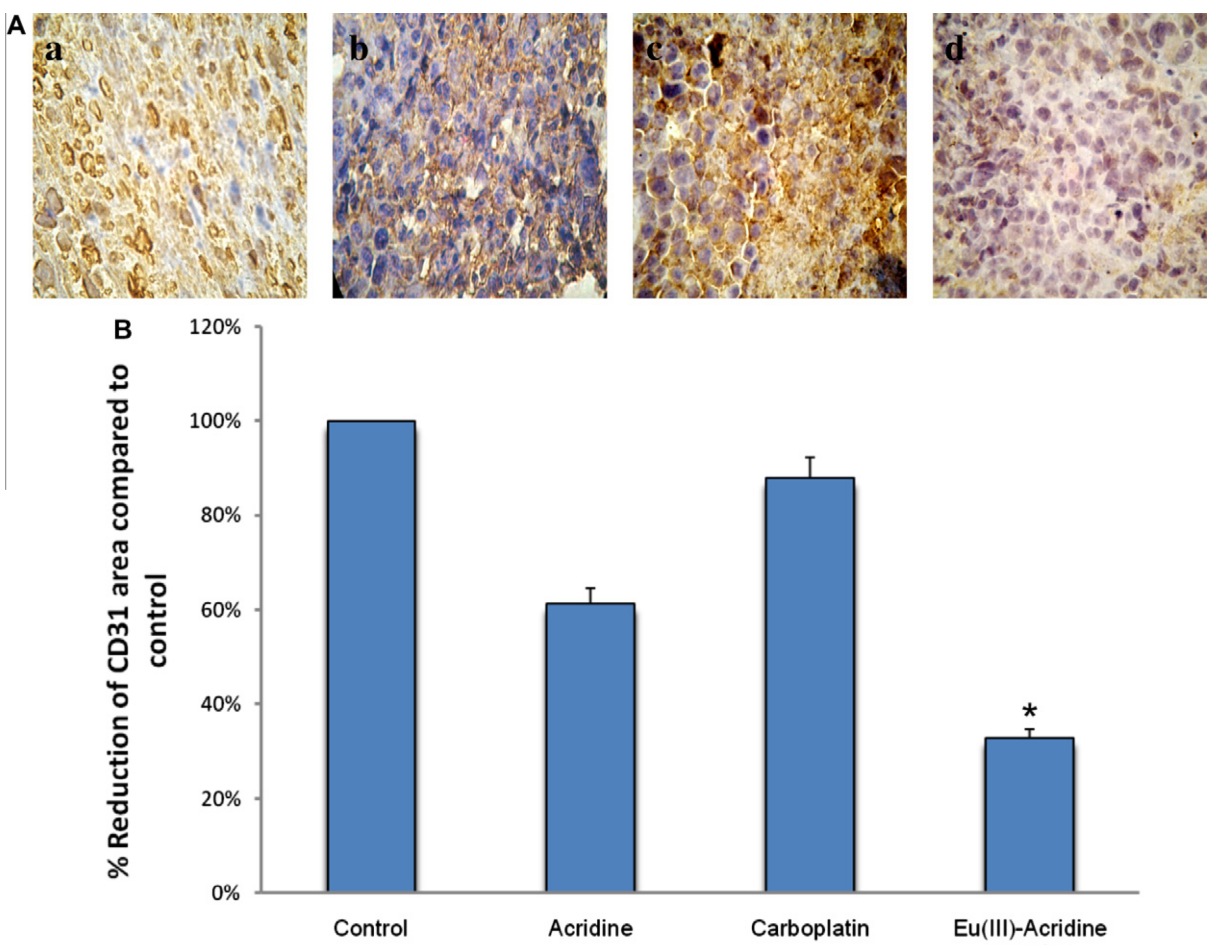

Figure 2. (A) Effect of treatment of $[Eu(9\text{-}ACA)_2(NO_3)]\cdot 2H_2O$ complex on CD31 assessed immunohistochemically on day 14 post-inoculation of EAC cells in Swiss albino mice (A) control; (B) 9-ACA treatment; (C) carboplatin treatment; (D) $[Eu(9\text{-}ACA)_2(NO_3)]\cdot 2H_2O$ complex treatment. (B) Statistical analysis of the $[Eu(9\text{-}ACA)_2(NO_3)]\cdot 2H_2O$ complex treatment on CD31 assessed immunohistochemically on day 14 post-implantation of EAC cells in Swiss albino mice. Data represent mean ± S.E.

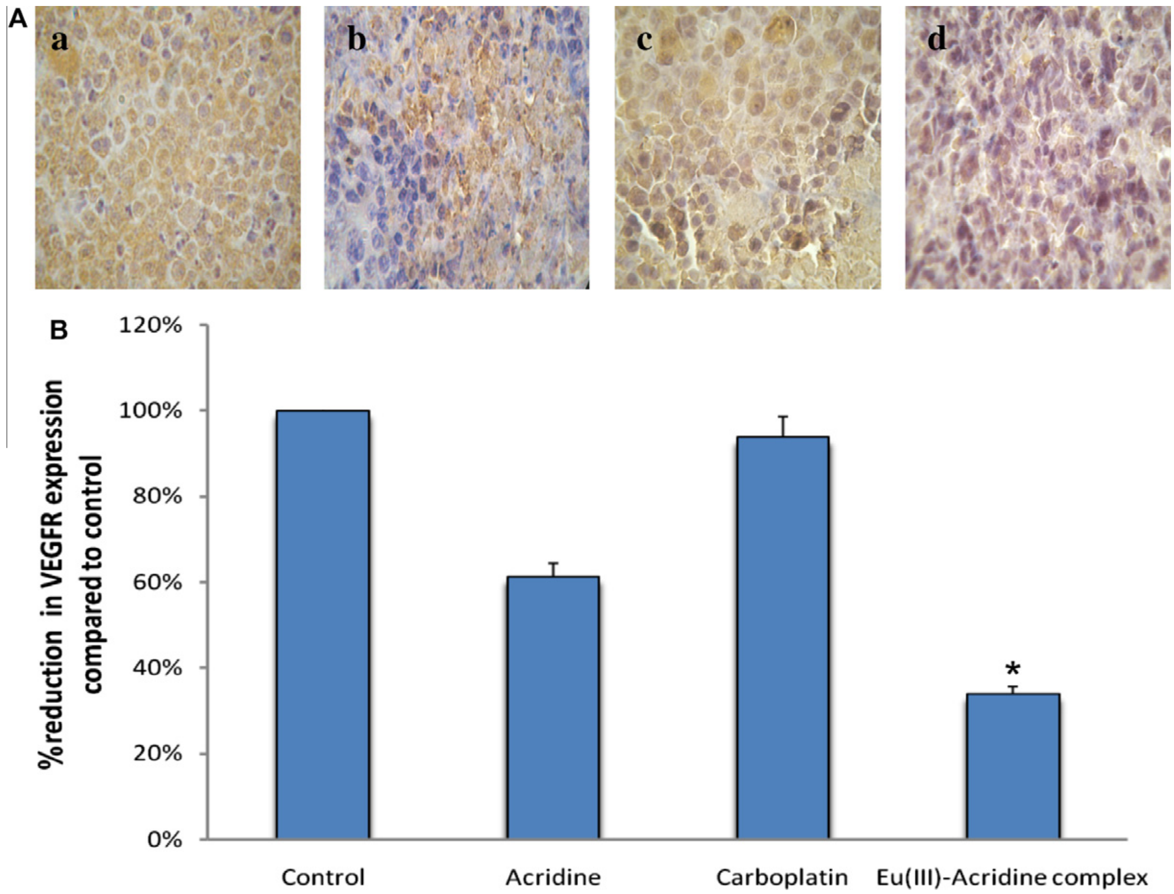

Figure 3. (A) Effect of treatment of $[Eu(9\text{-}ACA)_2(NO_3)]\cdot 2H_2O$ complex on VEGFR assessed immunohistochemically on day 14 post-inoculation of EAC cells in Swiss albino mice (A) control; (B) 9-ACA treatment; (C) carboplatin treatment; (D) $[Eu(9\text{-}ACA)_2(NO_3)]\cdot 2H_2O$ complex treatment. (B) Statistical analysis of $[Eu(9\text{-}ACA)_2(NO_3)]\cdot 2H_2O$ complex treatment on VEGFR assessed immunohistochemically on day 14 post-inoculation of EAC cells in Swiss albino mice. Data represent mean ± S.E.

Bis(acridine-9-carboxylate)-nitro-europium(III) dihydrate complex produced a highly significant ($P \leqslant 0.05$) reduction in microvessel density on day 14 compared to carboplatin, acridine-9-carboxylic acid, and untreated control animals (Fig. 2B)[32,33].

VEGF and its receptors, type-1 (Flt-1) and type-2 (Flk-1), have been implicated as key components in the vascularization of tumors. However, most of the VEGF angiogenic properties are mediated through interaction with VEGF receptor type-2.[25]

Sections of tumors from all untreated and treated groups were stained for VEGF receptor (Flk-1) to study tumor angiogenesis as shown in Figure 3A, a marked decrease of immunohistochemical staining of the Flk-1 was observed in the treated group in comparison to carboplatin, acridine-9-carboxylic acid, and untreated control animals.

Quantitative analysis indicated that, strong cytoplasmic expression of Flk-1 was observed in all EACs in the control and acridine-9-carboxylic acid only treated groups. Treatment with bis(acridine-9-carboxylate)-nitro-europium(III) dihydrate complex showed a highly significant reduction of the expression of Flk-1($P \leqslant 0.05$) as shown in Figure 3(B).

3.4. Effect of bis(acridine-9-carboxylate)-nitro-europium(III) dihydrate complex on caspase-3 expression

The caspases are a family of proteins that are one of the main executors of the apoptotic process. Out of all caspases, the caspase-3 is a frequently activated death protease and is indispensible for DNA fragmentation, chromatin condensation and the formation of apoptotic bodies in all the cell types tested.[34,35] To determine whether caspase-3 is involved in bis(acridine-9-carboxylate)-nitro-europium(III) dihydrate complex-induced apoptosis, caspase-3 expression was evaluated in all groups immunohistochemically. The result showed that treatment of EAC cells with bis(acridine-9-carboxylate)-nitro-europium(III) dihydrate complex gradually increased the caspase-3 expression (Fig. 4A). These results demonstrate the involvement of caspases-3 bis(acridine-9-carboxylate)-nitro-europium(III) dihydrate complex-induced apoptosis.

Quantitative analysis of intratumoral caspase-3 expression showed more than tenfold increase in the area percentage of the group treated with bis(acridine-9-carboxylate)-nitro-europium(III) dihydrate complex treated in comparison to carboplatin, acridine-9-carboxylic acid or untreated control animals ($P \leqslant 0.05$) as shown in Figure 4B.

3.5. Bis(acridine-9-carboxylate)-nitro-europium(III) dihydrate complex-induces DNA fragmentation of EAC cells

One of the hallmarks of apoptosis is the cleavage of chromosomal DNA into nucleosomal units. The caspases play an important role in this process by activating DNases, inhibiting DNA repair enzymes and breaking down structural proteins in the nucleus.[34,35] Induction of EAC cell apoptosis by bis(acridine-9-carboxylate)-nitro-europium(III) dihydrate complex, as shown in our results in vivo, explains the apoptotic action of bis(acridine-9-carboxylate)-nitro-europium(III) dihydrate complex towards EAC cells through caspase-3 activation. Bis(acridine-9-carboxylate)-nitro-europium(III) dihydrate complex treatment caused DNA fragmentations as was evident by the formation of DNA

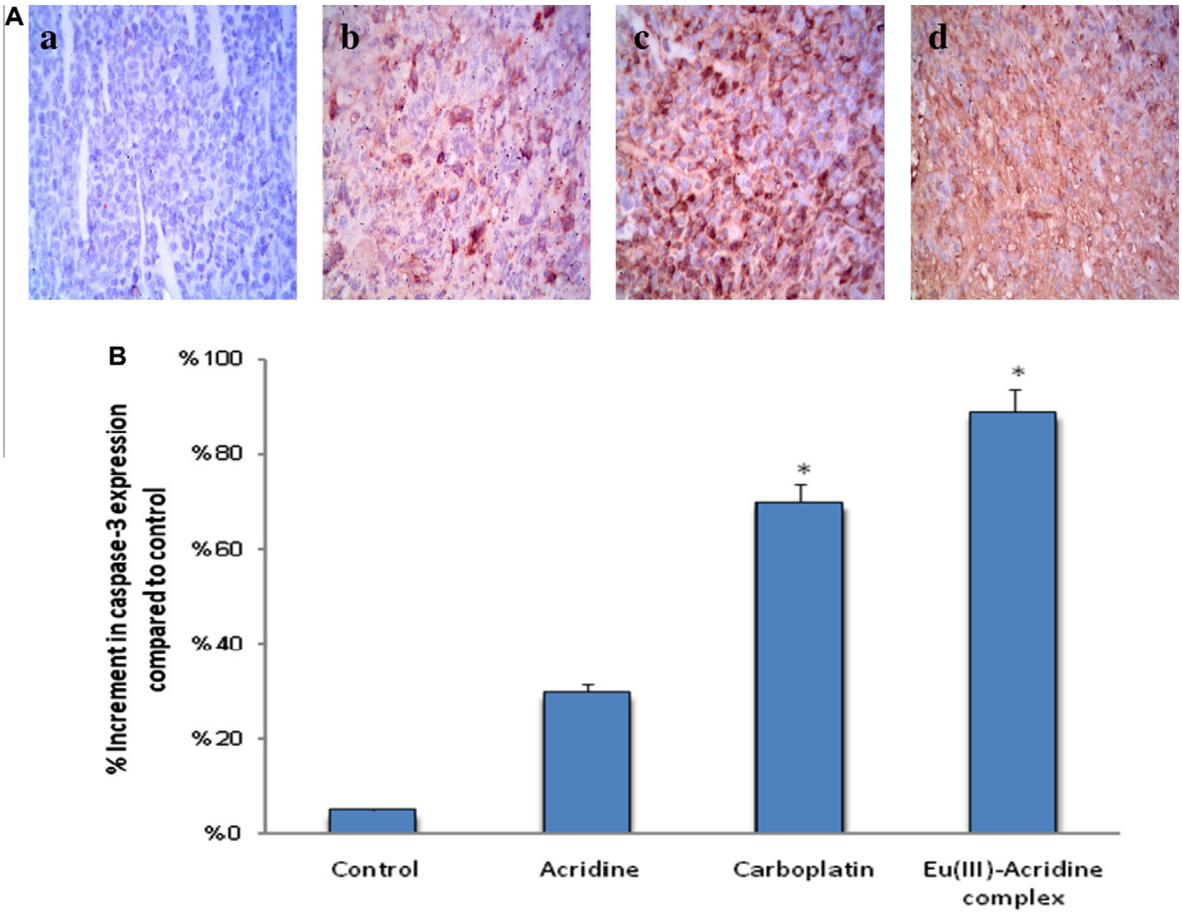

Figure 4. (A) Effect of treatment of $[Eu(9\text{-}ACA)_2(NO_3)]\cdot 2H_2O$ complex on caspase-3 assessed immunohistochemically on day 14 post-inoculation of EAC cells in Swiss albino mice (A) control; (B) 9-ACA treatment; (C) carboplatin treatment; (D) $[Eu(9\text{-}ACA)_2(NO_3)]\cdot 2H_2O$ complex treatment. (B) Statistical analysis of $[Eu(III)\text{-}(9\text{-}ACA)_2]$ complex treatment on caspase-3 assessed immunohistochemically on day 14 post-inoculation of EAC cells in Swiss albino mice. Data represent mean ± S.E.

Figure 5. Effect of $[Eu(9\text{-}ACA)_2(NO_3)]\cdot 2H_2O$ complex on genomic DNA of EAC cells, Lane 1: DNA of EAC untreated, Lane 2: DNA of EAC treated with $[Eu(9\text{-}ACA)_2(NO_3)].2H_2O$ complex.

ladder in EAC cells. This indicates the apoptotic role of Eu-complex in EAC cells (Fig. 5).

Figure 6 shows the data of DNA fragments analysis of the extracted DNA from EAC cells treated by bis(acridine-9-carboxylate)-nitro-europium(III) dihydrate complex for 7 days. Many peaks appeared and their migration time was compared to those of the standard DNA ladder marker 15–1000 bp. Peaks having a size of about 25–131 bp can be regarded as cleaved DNA fragments of short length while peaks having a size of about 156–800 bp are corresponding to one to six nucleosomes. Induction of apoptosis results in the formation of nucleosomes of DNA fragments with repeat lengths that may range from 160 to 240 bp.[36–38]

3.6. Cytotoxicity assay in vitro

The cytotoxicity in vitro assay for bis(acridine-9-carboxylate)-nitro-europium(III) dihydrate complex and acridine-9-carboxylatic ligand was assessed using the method of MTT reduction. Cisplatin was used as a positive control. After treatment of MCF-7 cell line for 24 h with each of complex and ligand in the range of concentration (1–50 μM). The inhibitory percentage against growth of cancer cells was determined. The cell viability (%) obtained with continuous exposure for 24 h and the cytotoxicity of complexes was found to be concentration-dependent. The cell viability decreased with increasing the concentrations of the complex.

As shown in Table 1 bis(acridine-9-carboxylate)-nitro-europium(III) dihydrate complex inhibited the growth MCF7 cell line with IC_{50} values of 14.3 ± 2.2 μM. The complex showed better

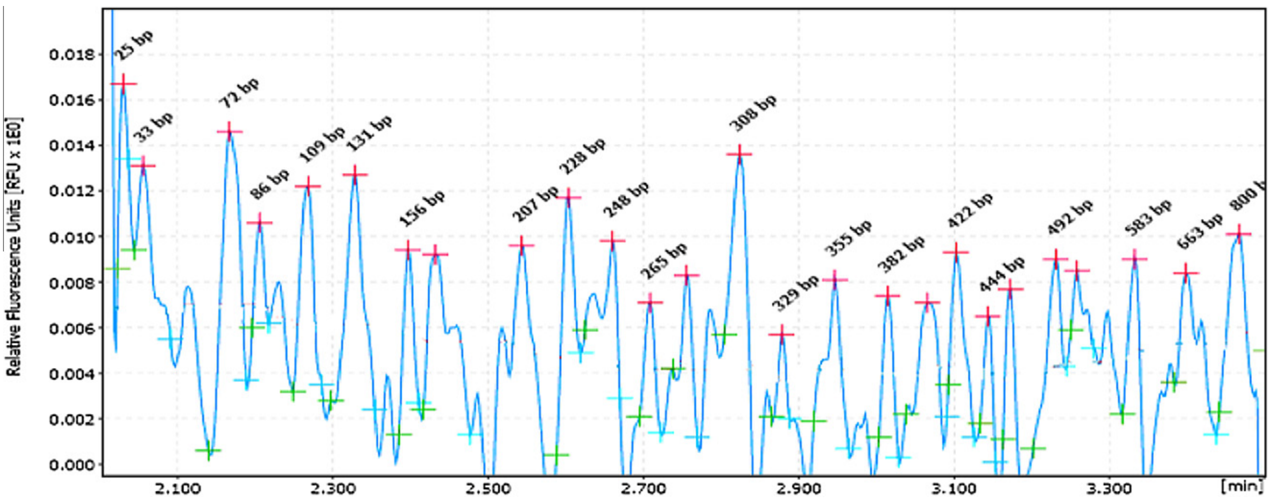

Figure 6. Capillary electropherogram of DNA extracted from EAC cells after treatment with $[Eu(9\text{-}ACA)_2(NO_3)]\cdot 2H_2O$ complex in vivo.

Table 1
In vitro anticancer screening of the synthesized Bis(acridine-9-carboxylate)-nitro-europium(III) dihydrate complex against human breast cell line (MCF7)

Compound	MCF7 IC_{50} (μM)
Cisplatin	12.7 ± 2.2
9-Acridine carboxylic acid	21.5 ± 3.1
Eu(III)-complex	14.3 ± 2.6

cytotoxicity compared to the ligand (IC_{50} = 21.5 ± 3.1) and closed cytotoxicity compared to the standard cisplatin (IC_{50} values of 12.7 ± 2.6 μM).

3.7. DNA binding studies

3.7.1. Fluorescent ethidium bromide displacement assay

The DNA-binding modes of the complex were further monitored by a fluorescent EB displacement assay. It is well known that EB can emit intense fluorescence in the presence of DNA, due to its strong intercalation between DNA base pairs. It was previously reported that the enhanced fluorescence can be quenched by the addition of a second molecule.[39] The quenching extent of fluorescence can be used to determine the extent of binding between the Eu(III)-complex and ds-DNA. As shown in Figure 7 the intensity of emission band at 601 nm of the EB-DNA system was reduced with the increasing of the concentration of the Eu(III)-complex, which indicated that the complex could displace EB from the EB-DNA system.[40,41]

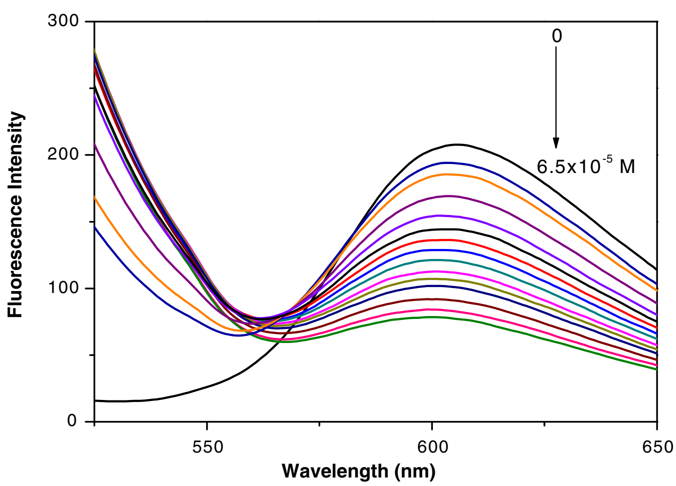

Figure 7. Fluorescence spectra of the combination of 5×10^{-4} EB and 10 μmol L^{-1} DNA in the absence and presence of increasing amounts of $Eu(9\text{-}ACA)_2(NO_3)]\cdot 2H_2O$ complex. λ_{ex} = 340 nm, λ_{em} = 525–650 nm. Arrows show the intensity changes upon increasing concentration of the complex.

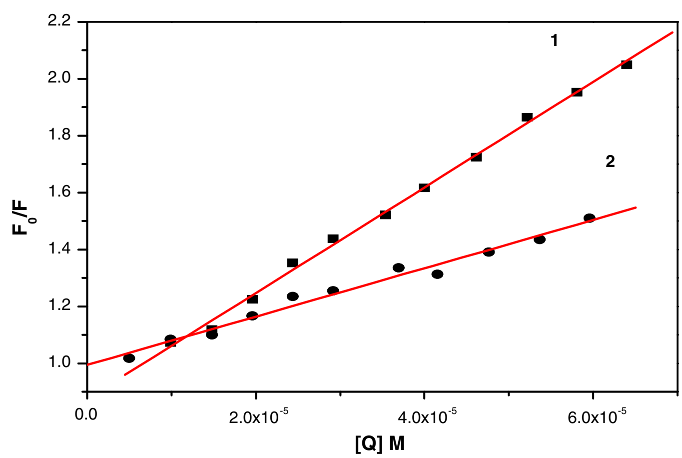

Figure 8. The Stern–Volmer quenching curves of EB + DNA with (1) $[Eu(9\text{-}ACA)_2(NO_3)]\cdot 2H_2O$ complex and (2) with acridine-9-carboxylic acid.

The quenching plots illustrate that the quenching by the complexes are in good agreement with the linear Stern–Volmer equation as displayed in Figure 8. According to the classical Stern–Volmer equation: $F_0/F = 1 + K_{sv}[Q]$, where F_0 and F represent the fluorescence intensities in the absence and presence of the complex, respectively, Q is the concentration ratio of the complex to DNA. K_{sv} is a linear Stern–Volmer quenching constant. The K_{sv} values for complex and 9-ACA are 1.8 (±0.5) × 10^4 M^{-1} and 0.8 (±0.4) × 10^4 M^{-1}, respectively.

3.8. Molecular docking of bis(acridine-9-carboxylate)-nitro-europium(III) dihydrate complex interaction Telomeric G-quadruplex DNA interaction

The promising results obtained from the Eu(III)-complex interaction with DNA stimulated us to further substantiate the results with molecular modeling studies and working on the only and recently metal complex crystal structure bound to human telomeric G-quadruplex DNA in PDB.

The first X-ray crystal structures of nickel(II) and copper(II) salphen metal complexes bound to a human telomeric G-quadruplex DNA has been recently precipitated in PDB (PDB code 3QSF). The formation of these quadruplexes in telomeres is responsible for maintaining length of telomeres and is involved in around 85% of all cancers. This is an active target of anticancer drug discovery.[42,43]

The docking studies revealed that the docking pattern of the proposed inhibitors is very close to that of the crystallized ligand suggesting a possible similar mode of action as shown in Figure 9. The molecule is interposed between the two DNA strands with its metal ion coordinated to a guanine oxygen and holding the two acridine rings in an imperfectly-planar conformation that allows hydrophobic interaction each with one of the two DNA strands. This pose also suggests a potential similar interaction at other sites of DNA through a bifunctional mechanism of action.

3.9. Molecular docking of bis(acridine-9-carboxylate)-nitro-europium(III) dihydrate complex interaction with tyrosine kinases

Several BCR-ABL crystal structure co-crystallized with known inhibitors were downloaded from PDB and their binding modes were investigated (PDB codes 3CS9, 3IK3, 3K5V, 3QRI, 3QRK). Study of the 3D structures revealed that all the inhibitors showed a similar binding mode with amino acids Glu 286, Thr 315, Met 318, Asp 381 are common residues in ligand binding. Docking of our proposed inhibitor showed that the compound also fitted well in the enzyme active site and established good interaction with the same key residues (Fig. 10).

The metal coordinated oxygen and the acridine nitrogen establish hydrogen bonds with Thr 315 side chain and Met 318 backbone, respectively. The other acridine nitrogen also forms hydrogen bond with Glu 286 side chain and is nearby for potential interaction with side chain and backbone of Asp 381 (Fig. 10).

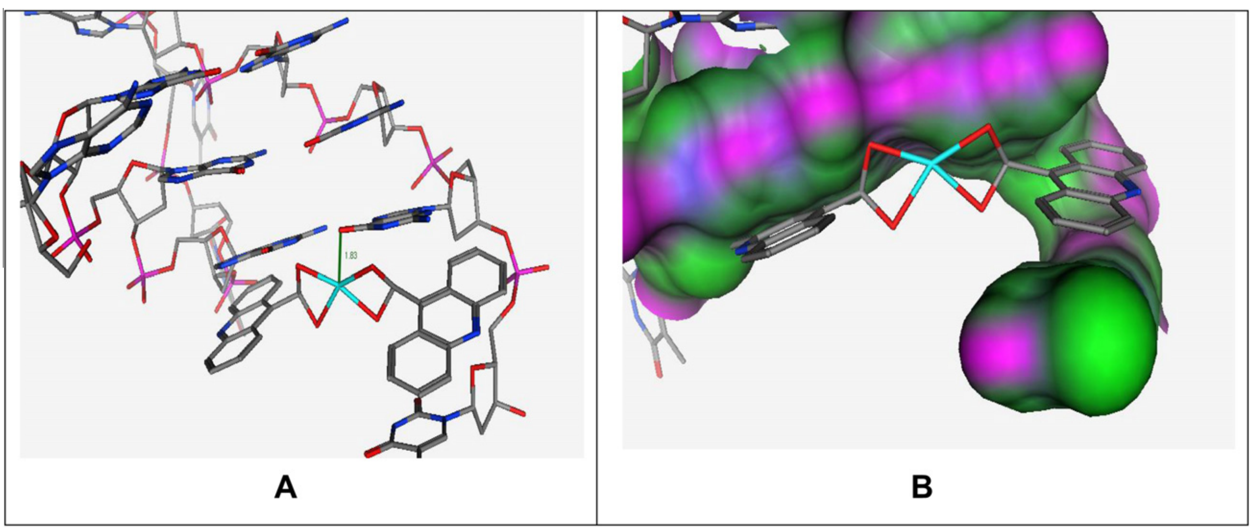

Figure 9. (A) Bis(acridine-9-carboxylate)-nitro-europium(III) dihydrate complex bind human telomeric G-quadruplex DNA. Distances in Á are indicated by green lines for potential bonding. (B) Bis(acridine-9-carboxylate)-nitro-europium(III) dihydrate complex binding to human telomeric G-quadruplex DNA represented as an electrostatic potential surface.

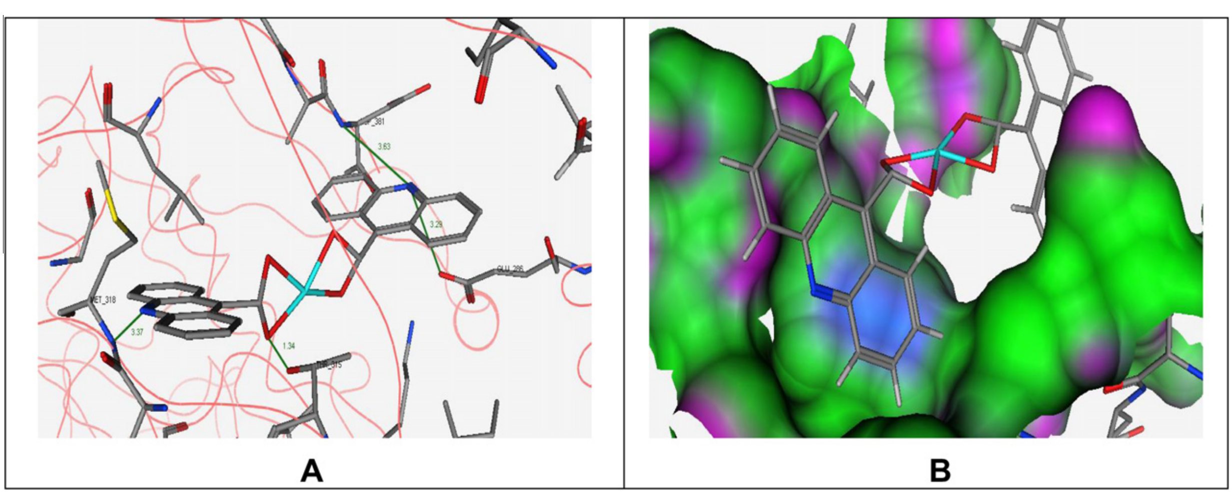

Figure 10. (A) Bis(acridine-9-carboxylate)-nitro-europium(III) dihydrate complex binds the active site of human BCR-ABL kinase. Distances in Á are indicated by green lines for potential hydrogen or coordination bonding. Backbones are represented as red lines. (B) Bis(acridine-9-carboxylate)-nitro-europium(III) dihydrate complex binding to the active site of human BCR-ABL kinase. Represented as an electrostatic potential surface.

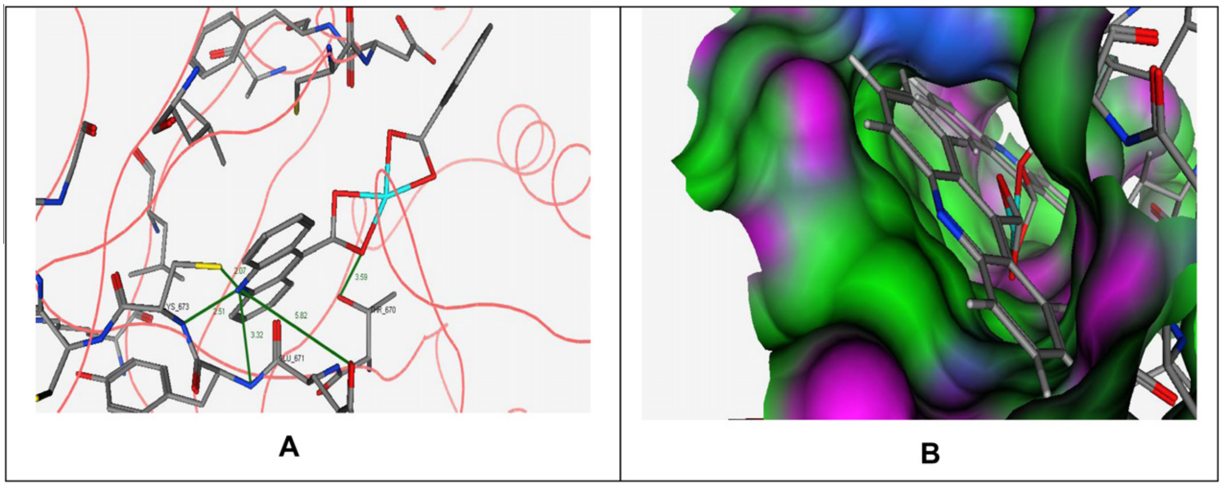

Figure 11. (A) Bis(acridine-9-carboxylate)-nitro-europium(III) dihydrate complex binds the active site of human c-kit kinase. Distances in Å are indicated by green lines for potential hydrogen or coordination bonding. Backbones are represented as red lines. (B) Bis(acridine-9-carboxylate)-nitro-europium(III) dihydrate complex binding to the active site human c-kit kinase. Represented as an electrostatic potential surface.

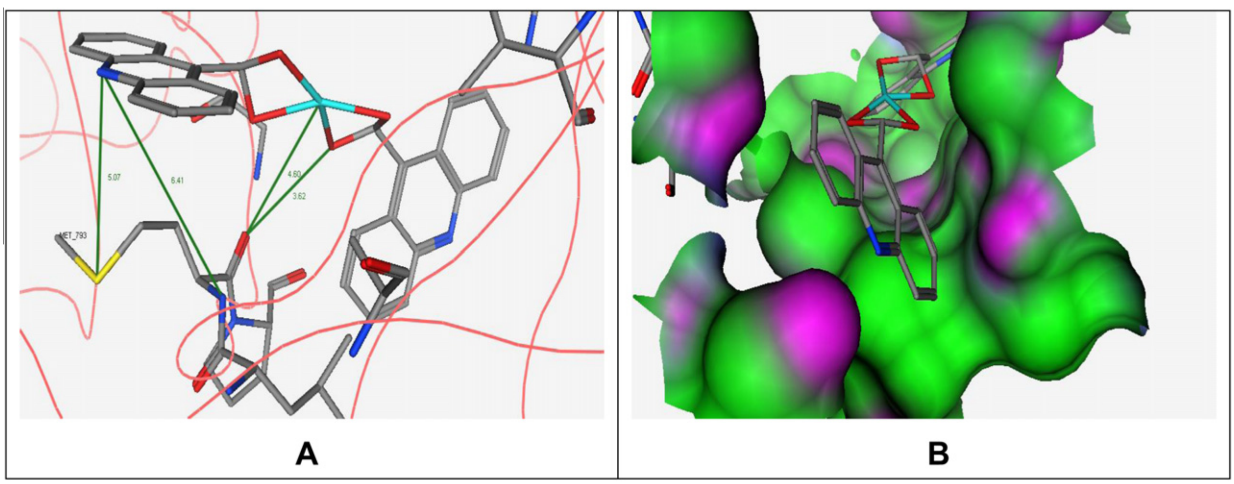

Figure 12. (A) Bis(acridine-9-carboxylate)-nitro-europium(III) dihydrate complex binds the active site of human EGFR kinase. Distances in Å are indicated by green lines for potential hydrogen or coordination bonding. Backbones are represented as red lines. (B) Bis(acridine-9-carboxylate)-nitro-europium(III) dihydrate complex binding to the active site of human EGFR kinase. Represented as an electrostatic potential surface.

Other residues involved in ligand binding at the active site include Val 258, lys 285, Val 289, Met 290, Phe 317, Phe 359, Phe 362.

The crystal structures for the c-kit enzyme found in the PDB include kit kinase in complex with sunitinib (PDB code 3G0E, 3G0F). The structures revealed Glu 671, Cys 673 as key residues in ligand binding. The enzyme active site accommodates the proposed inhibitor which establishes good interaction with the key residues in the binding pocket (Fig. 11). The acridine nitrogen forms hydrogen bond with Cys 673 backbone and side chain SH and Glu 671 backbone while the metal coordinated oxygen establishes hydrogen bond with Thr 670 side chain. The inhibitor is also held tightly in the active site through establishing hydrophobic interactions with Trp 557, Val 654, Cys 809, Asp 810.

Searching for the crystal structure of the EGFR kinase in the PDB revealed the 3D structure of the enzyme co-crystallised with different inhibitors (PDB codes 1XKK, 2ITW, 2ITY, 2JIU, 2JIV, 2RGP, 3BEL, 3IKA, 3LZB, 3POZ). The 3D structures revealed a key residue, Met 793, involved in binding all the inhibitors. The proposed inhibitor docked well in the EGFR kinase active site with a docking pattern that allowed possible interaction with Met 793. The metal and the metal coordinated oxygen are present at a distance from Met 793 backbone oxygen that could allow coordination bond and hydrogen bond formation, respectively, as shown in Figure 12.

Other residues holding the inhibitor tightly in the active site through hydrophobic interactions include Lys 721, Lys 745, Met 769, Arg 776, Asp 800, Leu 844, Thr 854. The surface of the BCR-ABL, c-kit kinase and EGFR kinase binding sites accommodate the compound without any steric collision (Fig. 10B, Fig. 11B and Fig 12B).

4. Discussion

The aim of this study was to determine if bis(acridine-9-carboxylate)-nitro-europium(III) dihydrate, a new synthesized lanthanum complex, possesses anti-angiogenic and apoptotic activity against an animal model of carcinogenesis.

First, new bis(acridine-9-carboxylate)-nitro-europium(III) dihydrate complex $[Eu(9\text{-}ACA)_2(NO_3)]\cdot 2H_2O$ was synthesized and characterized. Bis(acridine-9-carboxylate)-nitro-europium(III) dehydrate complex was synthesized by mixing ethanol solutions of acridine-9-carboxylic acid and the corresponding Eu(III) salt, in amounts equal to a ligand/metal molar ratio of 2:1. The new bis(acridine-9-carboxylate)-nitro-europium(III) dihydrate complex was characterized by different physicochemical methods: elemental analyses, ^{1}H NMR, ^{13}C NMR, FT-IR, Mass and TGA-DTA measurements. On the basis of the elemental analysis, thermal decomposition, IR, ^{1}H NMR, ^{13}C

NMR and mass spectra, the suggested structure of the complex is consistent with that shown in Scheme 1.

Our next step was to determine if our compounds have an effect on Ehrlich ascites carcinoma (EAC) in vivo. This is the first report to show that bis(acridine-9-carboxylate)-nitro-europium(III) dihydrate complex has antitumor activity as was evident by significant reduction of both the size of solid tumor and ascites formation in the current model. Treatment with acridine-9-carboxylic ligand showed a minimal effect on the growth of Ehrlich ascites carcinoma. The mechanism by which bis(acridine-9-carboxylate)-nitro-europium(III) dihydrate complex induces antitumor effect involved antiangiogenic activity. Tumor angiogenesis is the proliferation of a network of blood vessels that penetrates into cancerous growth. Angiogenesis is integral to tumor and metastasis. VEGF is a key player in angiogenesis and is over expressed in a number of cancers including cancer of colon, breast, lung and pancreas.[44,45] Therefore, agents that inhibit VEGF expression may have a great role in the treatment of cancer as the loss of VEGF expression in a tumor causes a dramatic decrease in vascular density and vascular permeability and increase tumor cell apoptosis.[7–9]

The antiangiogenic effect of bis(acridine-9-carboxylate)-nitro-europium(III) dihydrate was investigated in EAC in vivo in several ways. First, CD31, one of the most commonly used endothelial cell markers that highlight tumor blood vessels and reflect degree of angiogenesis was evaluated.[31,32] Our results revealed that tumors from animals treated with bis(acridine-9-carboxylate)-nitro-europium(III) dehydrate complex exhibited reduction of microvessel density. Second, immunohistochemical analysis showed that bis(acridine-9-carboxylate)-nitro-europium(III) dihydrate complex down-regulates the expression of Flk-1, which is closely linked with angiogenesis.

In addition to these results, we found that bis(acridine-9-carboxylate)-nitro-europium(III) dihydrate complex induced DNA apoptosis in EAC cells. The study of apoptosis of cancer cell has been a hotspot in the cancer therapy for a long time. Cell apoptosis is characterized by endogenous proteases activation, nuclear chromatin condensation, cytoplasmic shrinking, dilated endoplasmic reticulum, and membrane blebbing.[46,47] The fragmentation of DNA into nucleosomal units is caused by CAD enzyme, or caspase activated DNase. Normally CAD exists as an inactive complex with ICAD (inactive caspase activated DNase). During apoptosis, ICAD is cleaved by caspases, to release CAD followed by rapid fragmentation of the nuclear DNA. Therefore, most dramatic biochemical feature of apoptosis, is DNA fragmentation occurs as a result of cleavage of the cell's DNA at intervals of 160–240 base pairs (bp) which are the size of oligonucleosomes.[35–37]

Therefore, peaks with size 156–800 pb can be regarded as typical apoptotic DNA fragments, suggesting that the cells underwent apoptosis after been treated with bis(acridine-9-carboxylate)-nitro-europium(III) dihydrate complex for 7 days.

The effect of bis(acridine-9-carboxylate)-nitro-europium(III) dihydrate complex on Caspase-3 induction has also been studied to further interpretate the different possible mechanisms by which the compound can induce apoptosis and killing of the cancer cells. Caspases are currently considered as the central executioners of many, if not all, apoptotic pathways. It has been recently shown that drug-induced cytotoxicity involves proteases of the caspase family, because specific inhibitors of caspases prevented cell death after treatment with different anticancer agents.[48–51] The broad caspase inhibitor benzyloxycarbonyl-Val-Ala-Asp-fluoromethylketone prevented apoptosis and caspase activation in response to CD95 and drug treatment.[51] Caspase-3 is a member of the cysteine protease family, which plays a crucial role in apoptotic pathways by cleaving a variety of key cellular proteins. Caspase-3 can be activated by diverse death-inducing signals, including the chemotherapeutic agents.[52]

The activation of caspases has been mainly studied upon triggering of death receptors, such as CD95. Because apoptosis induced by anticancer drugs has been proposed to involve CD95/CD95 ligand interaction, we investigated the effect of bis(acridine-9-carboxylate)-nitro-europium(III) dihydrate complex on caspase-3 activation. The results of the immunohistochemistry caspase induction assay revealed that bis(acridine-9-carboxylate)-nitro-europium(III) dihydrate complex was much superior in caspase-3 induction compared to untreated cancer cell lines and cells treated with acridine. The concentration mean for caspase-3 expression was 44.9, 4.7 and 6.5 in case of bis(acridine-9-carboxylate)-nitro-europium(III) dihydrate complex treated cells, untreated cells and acridine treated cells, respectively.

In the described in vivo study, we have used carboplatin as a reference drug. This drug has been proven to be significantly less in antiangiogenic activity and VEGFR and CD31agonist activity Compared to our complex. However carboplatin was superior in reducing both tumor mass and tumor volume. Carboplatin and cisplatin were previously studied in a similar research study carried by members of the group and the results obtained were consistent with what we already had in these previous work.

Carboplatin was selected as a reference as it is one of the well-known metal containing standard anticancer agents.

The results of the in vitro assay demonstrated the cytotoxic effect of the synthesized complex and supported the results of the in vivo studies. The in vitro cytotoxicity assay showed a superior MCF cell growth inhibition compared to the acridine carboxylic acid and a relatively similar inhibition compared to the standard cisplatin.

The data obtained from ethidium bromide displacement suggest that the binding ability of complex with DNA is stronger than that of 9-ACA ligand. It indicates that complex could bond to DNA more easily than 9-ACA. The results indicate that the Eu-complex could intercalate DNA and squeeze EB from DNA double helix more easily.[53–55]

The promising results obtained from the Eu(III)-complex interaction with DNA stimulated us to further substantiate the results with molecular modeling studies and working on the only and recently metal complex crystal structure bound to human telomeric G-quadruplex DNA in PDB.

The results revealed good interaction of the complex with the crystallized DNA structure making the complex a new potential DNA chemotherapeutic intercalator.

Computer-assisted molecular docking was also employed to further explain and study the types of interactions that bis(acridine-9-carboxylate)-nitro-europium(III)dihydrate complex could establish with tyrosine kinase (TK). The new proposed drug blocks tyrosine kinase receptors namely VEGF-receptors, and therefore inhibit tyrosine kinase mediated angiogenesis. The biological results for VEGF-receptors inhibition are described above. In addition, they might also inhibit other tyrosine kinases within tumor cells which are linked to tumor cell growth and proliferation such as cKit and ABL. This means that this drug may block tumor cell growth directly, as well as by inhibiting angiogenesis.

TKs were implicated as oncogenes in animal tumors induced by retroviruses. The success of imatinib mesylate, an inhibitor of the BCR-ABL TK in chronic myeloid leukemia (CML) resulted in TKs now regarded as excellent targets for cancer chemotherapy. Three TKs was be considered in our molecular modeling studies to substantiate the activity of our proposed anticancer drug as possible inhibitor of tyrosine kinase. BCR-ABL, which has been implicated as the direct cause of CML[56], c-KIT which has been involved in gastrointestinal stromal tumors and other solid tumors such as some testicular seminomas and small-cell lung cancer[57,58], and EGFR which is overexpressed, mutated, or both in many solid tumors such as non-small-cell lung cancer and adenocarcinomas.[59]

The complex fitted well in the active site of the studied tyrosine kinases and establish different types of interaction including hydrogen and hydrophobic bonding suggesting that the compound is a potential inhibitor for the studied tyrosine kinases and confirming the results of the VEGFR tyrosine kinase inhibition study and subsequent antiangiogenic activity.

These results suggest that the bis(acridine-9-carboxylate)-nitro-europium(III) dihydrate complex could perform its antitumor activity through a dual mechanism of action; a DNA interchelation activity and a tyrosine kinase-mediated antiangiogenic activity.

For all of the above, our results showed that bis(acridine-9-carboxylate)-nitro-europium(III) dihydrate complex is a promising antitumor agent with a good apoptotic and anti-angiogenic activity.

5. Conclusion

Tumor angiogenesis is a promising target of cancer therapy. Based on this target, new organometallic complex bis(acridine-9-carboxylate)-nitro-europium(III) dihydrate complex was synthesized and characterized. In vivo anti-angiogenic and apoptotic potencies of bis(acridine-9-carboxylate)-nitro-europium(III) dihydrate complex against Ehrlich ascites carcinoma (EAC) cells were also demonstrated which makes the complex a promising chemotherapeutic agent based on the fact of synergy between apoptosis and anti-angiogenesis .

Antitumor activity indicated that bis(acridine-9-carboxylate)-nitro-europium(III) dihydrate complex showed potent antitumor activity against EAC cells by significant reduction of the tumor mass and volume in comparison to the 9-ACA treated and un-treated control groups.

In addition, our novel complex proved to exert an anti-angiogenic effect as shown by the reduction of microvessel density through, at least in part, the inhibition of VEGFR type-2. Also the apoptotic study exhibits that the new complex can effectively induce the apoptosis of EAC cells by up-regulation of Caspase-3 and formation of internucleosomal DNA ladder.

Combination of antiangiogenic with chemotherapeutic drugs especially DNA binding agents has higher efficiency in cancer treatment.[60] The results of biological activity of our compound showed a good antiangiogenic activity as clear from effect of bis(acridine-9-carboxylate)-nitro-europium(III) dihydrate complex on tumor angiogenesis and a good DNA binding activity through intercalation as showed in the fluorescent ethidium bromide displacement assay.

It is now obvious from what has been already discussed that the bis(acridine-9-carboxylate)-nitro-europium(III) dihydrate complex is superior to carboplatin in having a synergestic dual mechanism of action, through its tyrosine kinase mediated anti-angiogenesis and DNA and caspase3 mediated apoptosis and therefore is a potential powerful chemotherapeutic alternative.

In conclusion, the preliminary in vivo activity of the new complex showed that bis(acridine-9-carboxylate)-nitro-europium(III) dihydrate complex is a promising antitumor agent with a good antiangiogenic and apoptotic activity.

References and notes

1. Verheul, H. M.; Voest, E. E.; Schlingemann, R. O. *J. Pathol.* **2004**, *202*, 5.
2. Wu, H. C.; Huang, C. T.; Chang, D. K. *J. Cancer Mol.* **2008**, *4*, 37.
3. Rini, B. I. *Clin. Cancer Res.* **2007**, *13*, 1098.
4. Cao, Y. *Int. J. Biochem. Cell Biol.* **2001**, *33*, 357.
5. Son, Y. O.; Kook, S. H.; Choi, K. C.; Jang, Y. S.; Choi, Y. S.; Jeon, Y. M.; Kim, J. G.; Hwang, H. S.; Lee, J. C. *Eur. J. Pharmacol.* **2008**, *579*, 26.
6. Pan, M. H.; Lin, J. H.; Lin-Shiau, S. Y.; Lin, J. K. *Eur. J. Pharmacol.* **1999**, *381*, 171.
7. Hu, M.; Yang, J. L.; Teng, H., et al *BMC Cancer* **2008**, *8*, 306.
8. Belakavadi, M.; Salimath, P. B. *Mol. Cell. Biochem.* **2005**, *273*, 57.
9. Yasunori, K.; Rubin, T.; Laimute, T. S.; Timothy, L. C.; Steven, A.; Peter, H. *J. Clin. Invest.* **2000**, *106*, 1311.
10. Li, Y.; Yang, Z. Y.; Wang, M. F. *Eur. J. Med. Chem.* **2009**, *44*, 4585.
11. Wang, Z. M.; Lin, H. K.; Zhu, S. R.; Liu, T. F.; Zhou, Z. F.; Chen, R. T. *Anti-Cancer Drug Des.* **2000**, *15*, 405.
12. Saturnino, C.; Napoli, M.; Paolucci, G.; Bortoluzzi, M.; Popolo, A.; Pinto, A.; Longo, P. *Eur. J. Med. Chem.* **2010**, *45*, 4169.
13. Chen, Z. F.; Tan, M. X.; Liu, Y. C.; Peng, Yan; Wang, H. H.; Liu, H. G.; Liang, H. *J. Inorg. Biochem.* **2011**, *105*, 426.
14. Bacherikov, V. A.; Chang, J. Y.; Lin, Y. W.; Chen, C. H.; Pan, W. Y.; Dong, H.; Lee, R. Z.; Chouc, T. C.; Sua, T. L. *Bioorg. Med. Chem.* **2005**, *13*, 6513.
15. Sanchez, I.; Reches, R.; Caignard, D. H.; Renard, P.; Pujol, M. D. *Eur. J. Med. Chem.* **2006**, *41*, 340.
16. Asche, C.; Dumy, P.; Carrez, D.; Croisy, A.; Demeunynck, M. *Bioorg. Med. Chem. Lett.* **2006**, *16*, 1990.
17. Bouffier, L.; Baldeyrou, B.; Hildebrand, M. P.; Lansiaux, A.; Cordonnier, M. H. D.; Carrez, D.; Croisy, A.; Renaudet, O.; Dumy, P.; Demeunynck, M. *Bioorg. Med. Chem.* **2006**, *14*, 7520.
18. Wang, S. S.; Lee, Y. J.; Hsu, C. D.; Chang, H. O.; Yin, W. K.; Chang, L. S.; Choub, S. Y. *Bioorg. Med. Chem.* **2007**, *15*, 735.
19. Mauel, J.; Denny, W.; Gamage, S.; Ransijn, A.; Wojcik, S.; Figgit, D.; Ralph, R. *Antimicrob. Agents Chemother.* **1993**, *37*, 991.
20. Anderson, M. O.; Sherrill, J.; Madrid, P. B.; Liou, A. P.; Weisman, J. L.; Risi, D. J. L.; Guy, R. K. *Bioorg. Med. Chem.* **2006**, *14*, 334.
21. Chen, Y. L.; Chen, I. L.; Lu, C. M.; Tzeng, C. C.; Tsao, L. T.; Wang, J. P. *Bioorg. Med. Chem.* **2003**, *11*, 3921.
22. Cope, H.; Mutter, R.; Heal, W.; Pascoe, C.; Brown, P.; Pratt, S.; Chen, B. *Eur. J. Med. Chem.* **2006**, *41*, 1124.
23. Atwell, G. J.; Rewcastle, G. W.; Baguley, B. C.; Denny, W. A. *J. Med. Chem.* **1987**, *30*, 664.
24. Lazarus, H.; Tegeler, W.; Mazzone, H.; Leroy, J.; Boone, B.; Foley, G. *Cancer Chemother. Rep.* **1966**, *50*, 543.
25. El-Azab, M.; Hishe, H.; Moustafa, Y.; El-Awady, E. *Eur. J. Pharmacol.* **2011**, *652*, 7.
26. Bromberga, N.; Dreyfussb, J. L.; Regatierib, C. V.; Palladinob, M. V.; Durana, N.; Naderb, H. B.; Haund, M.; Justob, G. Z. *Chem. Biol. Interact.* **2010**, *168*, 43.
27. Prabhakar, B. T.; Khanum, S. A.; Jayashree, K.; Salimath, B. P.; Shashikanthc, S. *Bioorg. Med. Chem.* **2006**, *14*, 435.
28. Pal, S.; Choudhuri, T.; Chattopadhyay, S.; Bhattacharya, A.; Datta, G. K.; Das, T.; Sa, G. *Cell Biochem. Biophys. Res. Commun.* **2001**, *288*, 658.
29. Mosmann, T. *J. Immunol. Methods* **1983**, *65*, 55.
30. Molecular Operating Environment 2008.10 (MOE), Chemical Computing Group Inc., Montreal, Quebec, Canada, http://www.chemcomp.com.
31. PDB; protein data bank, 2011, http://www.rcsb.org/pdb.
32. Müller, A. M.; Hermanns, M. I.; Skrzynski, C.; Nesslinger, M.; Müller, K. M.; Kirkpatrick, C. J. *Exp. Mol. Pathol.* **2002**, *72*, 221.
33. Wang, D.; Stockard, C. R.; Harkins, L.; Lott, P.; Salih, C.; Yuan, K.; Buchsbaum, D.; Hashim, A.; Zayzafoon, M.; Hardy, R.; Hameed, O.; Grizzle, W.; Siegal, G. P. *Biotech. Histochem.* **2008**, *83*, 179.
34. Enari, M.; Sakahira, H.; Yokoyama, H.; Okawa, K.; Iwamatsu, A.; Nagata, S. *Nature* **1998**, *391*, 43–50.
35. Porter, A. G.; Janicke, R. U. *Cell Death Differ.* **1999**, *6*, 99.
36. Yu, S. B.; Geng, J.; Zhou, P.; Feng, A. R.; Chen, X. D.; Hu, J. M. *J. Pharm. Biomed. Anal.* **2007**, *43*, 816.
37. Minjie, X.; Wei, W.; Zhou, Z.; Yongfei, Y. *J. Pharm. Biomed. Anal.* **2005**, *39*, 853.
38. Valenzuela, M. T.; Nunez, M. I.; Guerrero, M. R.; Villalobos, M.; Almodovar, J. M. R. *J. Chromatogr., A* **2000**, *871*, 321.
39. Barton, J. K.; Raphael, A. L. *J. Am. Chem. Soc.* **1984**, *106*, 2466.
40. Zeng, Y. B.; Yang, N.; Liu, W. S.; Tang, N. *J. Inorg. Biochem.* **2003**, *97*, 258.
41. Liu, J.; Zhang, T.; Lu, T.; Qu, L.; Zhou, H.; Zhang, Q.; Ji, L. *J. Inorg. Biochem.* **2002**, *91*, 269.
42. Campbell, N. H.; Abd Karim, N. H.; Parkinson, G. N.; Gunaratnam, M.; Petrucci, V.; Todd, A. K.; Vilar, R.; Neidle, S. *J. Med. Chem.* **2012**, *1*, 209.
43. Zhang, J.; Zhang, F.; Li, H.; Liu, C.; Xia, J.; Ma, L.; Chu, W.; Zhang, Z.; Chen, C.; Li, S.; Wang, S. *Curr. Med. Chem.* **2012**, *18*, 2957.
44. Miller, K. D.; Sweeney, C. J.; Sledge, G. W. *J. Clin. Oncol.* **2001**, *19*, 1195.
45. Semenza, G. L. *Cancer Metastasis Rev.* **2000**, *19*, 59.
46. Earnshaw, W. C.; Martins, L. M.; Kaufmann, S. H. *Annu. Rev. Biochem.* **1999**, *68*, 383.
47. Saraste, A.; Pulkki, K. *Cardiovasc. Res.* **2000**, *45*, 528.
48. Zhu, H.; Fearnhead, H. O.; Cohen, G. M. *FEBS Lett.* **1995**, *374*, 303.
49. Chen, Z.; Naito, M.; Mashima, T.; Tsuruo, T. *Cancer Res.* **1996**, *56*, 5224.
50. Datta, R.; Banach, D.; Kojima, H.; Talanian, R. V.; Alnemri, E. S.; Wong, W. W.; Kufe, D. W. *Blood* **1996**, *88*, 1936.
51. Los, M.; Herr, I.; Friesen, C.; Fulda, S.; Schulze-Osthoff, K.; Debatin, K. M. *Blood* **1997**, *90*, 3118.
52. Devarajan, E.; Sahin, A. A.; Chen, J. S., et al *Oncogene* **2002**, *21*, 8843.
53. Baguley, B.; Bret, M. *Biochem* **1984**, *23*, 937.
54. Satyanarayana, S.; Dabrowiak, J.; Chaires, J. *Biochem* **1993**, *32*, 2573.
55. Zhu, W. Z.; Lin, Q. Y.; Lu, M.; Hu, R. D.; Zheng, X. L.; Cheng, J. P.; Wang, Y. Y. *J. Fluoresc.* **2009**, *19*, 857.
56. Van Etten, R. A.; Shannon, K. M. *Cancer Cell* **2004**, *6*, 547.
57. Hirota, S.; Isozaki, K.; Moriyama, Y., et al *Science* **1998**, *279*, 577.
58. Rubin, B. P.; Singer, S.; Tsao, C., et al *Cancer Res.* **2001**, *61*, 8118.
59. Mendelsohn, J.; Baselga, J. *Oncogene* **2000**, *19*, 6550.
60. Ma, J.; Waxman, D. J. *Mol. Cancer Ther.* **2008**, *7*, 3670.